

FIG. 1. Ratio of propagated NSI to SI atmospheric fluxes at detector level. We set  $\epsilon_{\mu\tau} = -0.05$ , and all other NSI parameters to zero. Dotted (dashed) lines show the regions in which 99% of the DeepCore (IceCube) MC events are contained. *Left panel:* Propagated fluxes of  $\nu_e$  and  $\nu_\tau$  neutrinos and anti-neutrinos. *Right panel:* Propagated fluxes of  $\nu_\mu$  neutrinos and anti-neutrinos

## I. METHODOLOGY

The neutrino flux at the detector is calculated by propagating the atmospheric neutrino flux [1] through the Earth by solving the Schrödinger equation for varying density. The Earth density profile is taken from the PREM [2]. The baseline for a given trajectory is determined using an average neutrino production height of 15 km and an Earth radius of 6371 km.

The oscillation probability  $P_{\alpha\beta}$  acts as a weight to the atmospheric flux, yielding the propagated flux at detector level for flavor  $\beta$  as

$$\phi_\beta^{\text{det}} = \sum_\alpha P_{\alpha\beta} \phi_\alpha^{\text{atm}}, \quad (1)$$

where we sum over the initial lepton flavors  $\alpha \in \{e, \mu, \bar{e}, \bar{\mu}\}$ . To illustrate the impact of  $\epsilon_{\mu\tau}$  on both probability and flux level, we plot the oscillograms resulting from Eq.1 in Fig. 1. In the left panel, we have marked the region in which 99% of the DeepCore cascade events originating from  $\nu_e$  and  $\nu_\tau$  fluxes are contained. In the right panel, we show the two regions in which 99% of the IceCube and DeepCore track events originating from  $\nu_\mu$  fluxes are contained. Starting with the  $\nu_\mu$  flux ratio, we see that the only clear signal discernible to the IceCube detector is a flux deficiency of a factor of  $\sim 10^2$  from core-crossing neutrinos within a zenith range of  $\cos(\theta_z^{\text{true}}) > -0.87$ . DeepCore, on the other hand, observes multiple fringes of flux surpluses with a factor  $\sim 10^1$ . The strongest surplus at 20 GeV is very weakly zenith dependent, a stark contrast to the energy-independent but zenith-sensitive IceCube deficiency.

For the fluxes which drives cascades, we have to resort to the DeepCore detector alone. Here we see a somewhat weaker signal, this time a zenith-independent deficiency.

### A. IceCube

The event rate for each bin reads

$$N_{ij} = T \int_{(\cos \theta_z^r)_i}^{(\cos \theta_z^r)_{i+1}} d \cos \theta_z^r \int_{E_j^r}^{E_{j+1}^r} dE^r \int_0^\pi R(\theta^r, \theta^t) d \cos \theta^t \int_0^\infty R(E^r, E^t) dE^t \times \left[ \sum_\beta \phi_\beta^{\text{det}} A_\beta^{\text{eff}} \right], \quad (2)$$

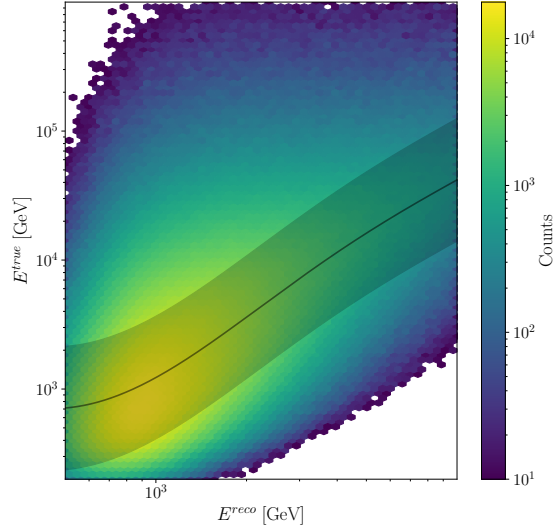


FIG. 2. Relationship between the true and reconstructed muon energy in the IceCube MC sample [4]. Shaded area shows the 99.9th percentile limits predicted by the regressor trained on this set.

where  $T$  is the live time of the detector, and  $A_{\beta}^{\text{eff}}$  its effective area for flavor  $\beta$ . We use the effective area of the 86 string configuration made public by the IceCube collaboration [3].  $R(x^r, x^t)$  is a resolution function, which is responsible for the smearing between the reconstructed and true parameters  $x^r$  and  $x^t$ , respectively. We assume a log-normal distribution, giving it the form

$$R(x^r, x^t) = \frac{1}{\sqrt{2\pi}\sigma_{x^r}x^r} \exp\left[-\frac{(\log x^r - \mu(x^t))^2}{2\sigma_{x^r}^2}\right]. \quad (3)$$

As seen in Fig. 2, the energy reconstruction is biased. To model this relationship between  $E^{\text{true}}$  and  $E^{\text{reco}}$ , we train a Gaussian process regressor on the dataset [4], from which we can extract a predicted mean and standard deviation for a given  $E^{\text{reco}}$ . We then take the  $E^{\text{true}}$  points of the 99th percentile of each distribution to obtain the limits of  $E^{\text{true}}$  at which to integrate over. We have no angular resolution function since the angle resolution in Icecube for track-like events is less than  $2^\circ$ , making  $\cos(\theta_z^{\text{true}})$  coincide with  $\cos(\theta_z^{\text{reco}})$  for our study [5]. The data is from the IC86 sterile analysis [5].

## B. DeepCore

In this part, we use the publically available DeepCore data sample [6] which is an updated version of what was used by the IceCube collaboration in a  $\nu_{\mu}$  disappearance analysis [7].

The detector systematics include ice absorption and scattering, and overall, lateral, and head-on optical efficiencies of the DOMs. They are applied as correction factors using the best-fit points from the DeepCore 2019  $\nu_{\tau}$  appearance analysis [8].

The data include 14901 track-like events and 26001 cascade-like events, both divided into eight  $\log_{10} E^{\text{reco}} \in [0.75, 1.75]$  bins, and eight  $\cos(\theta_z^{\text{reco}}) \in [-1, 1]$  bins. Each event has a Monte Carlo weight  $w_{ijk,\beta}$ , from which we can construct the event count as

$$N_{ijk} = C_{ijk} \sum_{\beta} w_{ijk,\beta} \phi_{\beta}^{\text{det}}, \quad (4)$$

where  $C_{k\beta}$  is the correction factor from the detector systematic uncertainty and  $\phi_{\beta}^{\text{det}}$  is defined as Eq. 1. We have now substituted the effect of the Gaussian smearing by treating the reconstructed and true quantities as a migration matrix.

The oscillation parameters used on our DeepCore simulations are from the best-fit in the global analysis in [9]:  $\theta_{12} = 33.44^\circ$ ,  $\theta_{13} = 8.57^\circ$ ,  $\Delta m_{21}^2 = 7.42 \text{ eV}^2$ , and we marginalize over  $\Delta m_{31}^2$  and  $\theta_{23}$ .

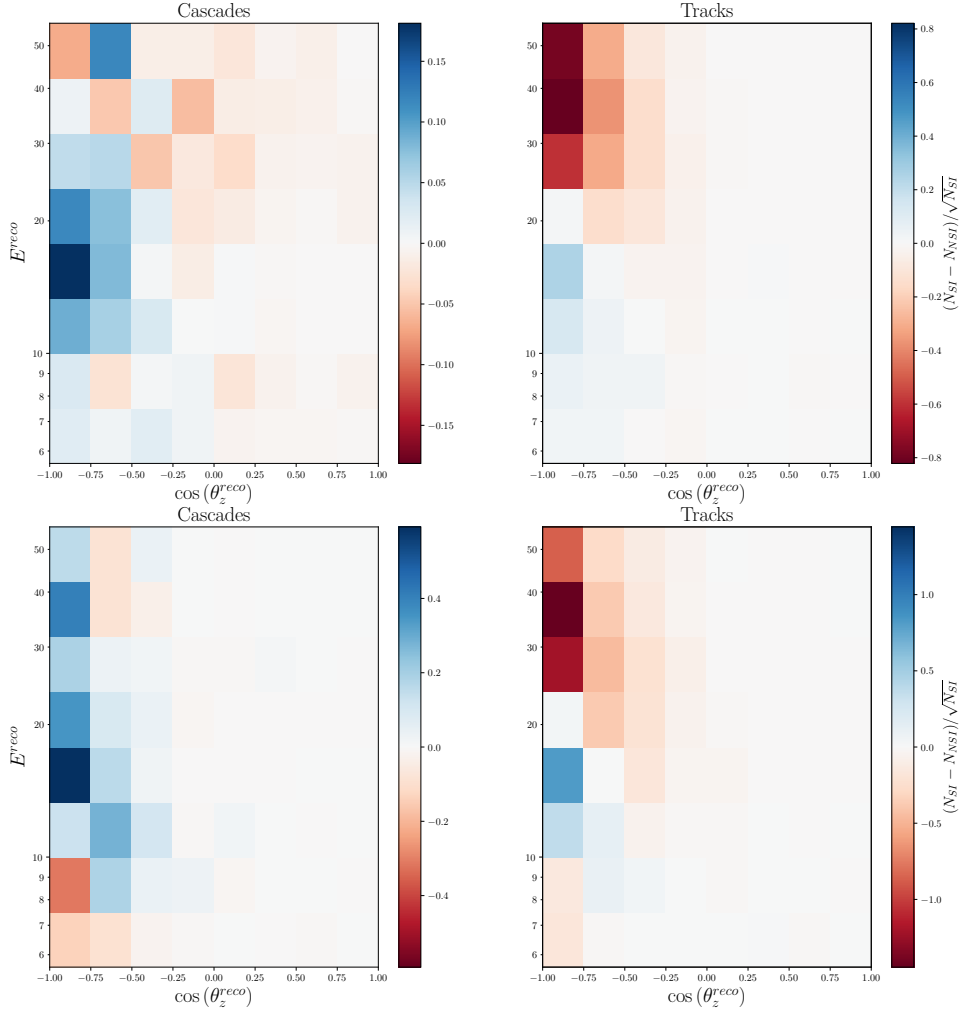


FIG. 3. Expected pulls of predicted event numbers for DeepCore and PINGU after 3 years. We compare the NSI event count with  $\epsilon_{\mu\tau} = -0.05$  to the standard interaction count

We plot the event pull  $(N_{NSI} - N_{SI})/\sqrt{N_{SI}}$  where  $N_{(N)SI}$  are the numbers of expected events assuming (non-)standard interactions in Fig. 3. This gives the normalized difference in the number of expected events at the detector, and illustrates the expected sensitivity of DeepCore for the NSI parameters.

### C. PINGU

The methodology behind the PINGU simulations are the same as with our DeepCore study IB. We use the public MC [10], which allows us to construct the event count as in Eq. 4. However, since no detector systematics is yet modelled for PINGU, the correction factors  $C_{ijk}$  are all unity. As with the DeepCore data, the PINGU MC is divided into eight  $\log_{10} E^{reco} \in [0.75, 1.75]$  bins, and eight  $\cos(\theta_z^{reco}) \in [-1, 1]$  bins for both track- and cascade-like events. We generate "data" by predicting the event rates at PINGU with the following best-fit parameters from [9], except for the CP-violating phase which is set to zero for simplicity.

$$\begin{aligned} \Delta m_{21}^2 &= 7.42 \times 10^{-5} \text{ eV}^2, \quad \Delta m_{31}^2 = 2.517 \times 10^{-3} \text{ eV}^2, \\ \theta_{12} &= 33.44^\circ, \quad \theta_{13} = 8.57^\circ, \quad \theta_{23} = 49.2^\circ, \quad \delta_{CP} = 0. \end{aligned} \tag{5}$$

## II. RESULTS

For our analyses, we define our  $\chi^2$  as

$$\chi^2(\hat{\theta}, \alpha, \beta, \kappa) = \sum_{ijk} \frac{(N^{\text{th}} - N^{\text{data}})_{ijk}^2}{(\sigma_{ijk}^{\text{data}})^2 + (\sigma_{ijk}^{\text{syst}})^2} + \frac{(1 - \alpha)^2}{\sigma_\alpha^2} + \frac{\beta^2}{\sigma_\beta^2} \quad (6)$$

where we minimize over the model parameters  $\hat{\theta} \in \{\Delta m_{31}^2, \theta_{23}, \epsilon', \epsilon_{\mu\tau}\}$ , the penalty terms  $\alpha$  and  $\beta$ , and the free parameter  $\kappa$ .  $N_{ijk}^{\text{th}}$  is the expected number of events from theory, and  $N_{ijk}^{\text{data}}$  is the observed number of events in that bin. We set  $\sigma_\alpha = 0.25$  as the atmospheric flux normalization error, and  $\sigma_\beta = 0.04$  as the zenith angle slope error [1]. The observed event number has an associated Poissonian uncertainty  $\sigma_{ijk}^{\text{data}} = \sqrt{N_{ijk}^{\text{data}}}$ .

For IceCube, the event count takes the form

$$N_{ijk}^{\text{th}} = \alpha [1 + \beta(0.5 + \cos(\theta_z^{\text{eco}})_i)] N_{ijk}(\hat{\theta}), \quad (7)$$

with  $N_{ijk}(\hat{\theta})$  from Eq. 2. Here, we allow the event distribution to rotate around the median zenith of  $-0.5$ .

For DeepCore and PINGU, the event count takes the form

$$N_{ijk}^{\text{th}} = \alpha [1 + \beta \cos(\theta_z^{\text{eco}})_i] N_{ijk}(\hat{\theta}) + \kappa N_{ijk}^{\mu_{\text{atm}}}, \quad (8)$$

with  $N_{ijk}(\hat{\theta})$  from Eq. 4.  $N_{ijk}^{\mu_{\text{atm}}}$  is the muon background, which is left to float freely in the DeepCore analysis. The background at PINGU can be considered negligible to first order [10], and we thus put  $\kappa = 0$  when calculating the PINGU  $\chi^2$ . For IceCube, we set  $\sigma_{ijk}^{\text{syst}} = f \sqrt{N_{ijk}^{\text{data}}}$ . For DeepCore, we use the provided systematic error distribution which accounts for both uncertainties in the finite MC statistics and in the data-driven muon background estimate [6].

First, we set all standard oscillation parameters to their current best-fit values of Eq. 5, except for  $\Delta m_{31}^2$  and  $\theta_{23}$ , which we marginalize over their  $3\sigma$  ranges of  $2.435 \times 10^{-3}$  to  $2.598 \times 10^{-3}$  eV<sup>2</sup> and  $40.1$  to  $51.7^\circ$  respectively.

For the joint analysis, we follow the parameter goodness-of-fit prescription [12] and construct the joint  $\chi^2$  as

$$\chi_{\text{joint}}^2 = \chi_{\text{IC}}^2 + \chi_{\text{DC}}^2 + \chi_{\text{P}}^2 - \chi_{\text{IC},\text{min}}^2 - \chi_{\text{DC},\text{min}}^2 - \chi_{\text{P},\text{min}}^2 \quad (9)$$

with test statistic  $\chi_{\text{joint},\text{min}}^2$ .

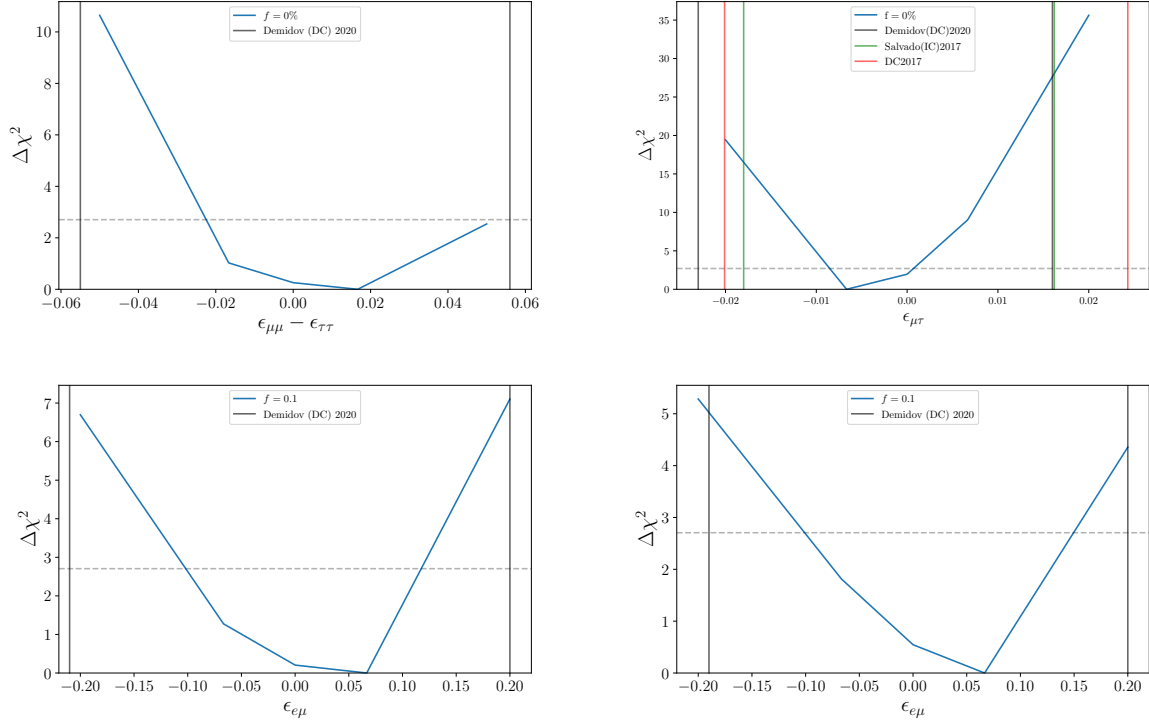


FIG. 4. The expected values of  $\Delta\chi^2$  after three years of PINGU data.  $\Delta m_{31}^2$  and  $\theta_{23}$  and have been marginalized out, and all NSI parameters not shown in each plot are set to zero.

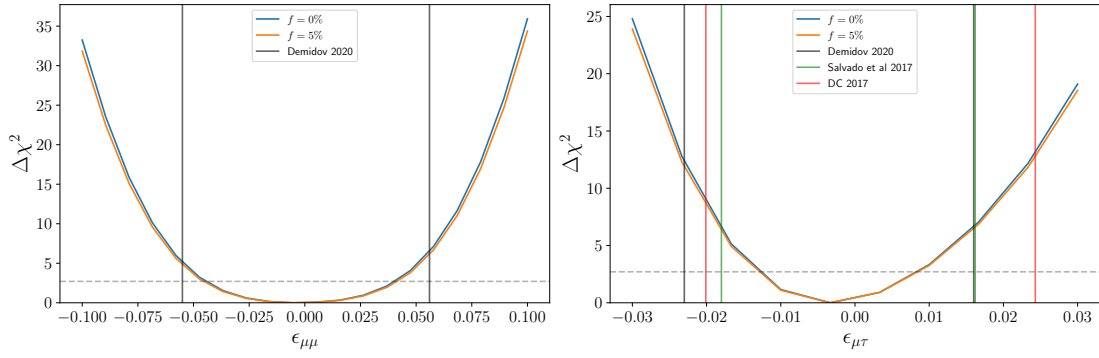


FIG. 5. The expected values of  $\Delta\chi^2$  after three years of PINGU data.  $\Delta m_{31}^2$  and  $\theta_{23}$  and have been marginalized out, and all other NSI parameters are set to zero. The black lines show the 90% credibility region from [11]

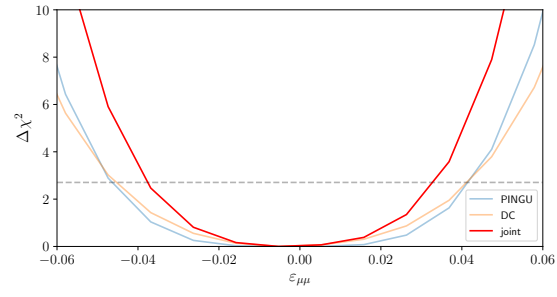


FIG. 6.

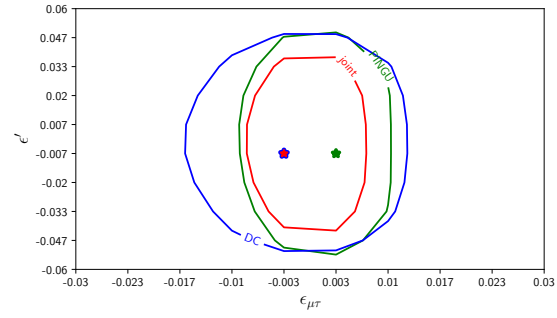


FIG. 7.

| DeepCore (2017)  | Demidov (2020) DC analysis  | This DC+PINGU analysis  |
|--|---|---|
| ✓ Honda atmospheric fluxes   | ✓ Honda atmospheric fluxes  | ✓ Honda atmospheric fluxes  |
| × Only look at tracks and $\epsilon_{\mu\tau}$                     | ✓ Looks at tracks + cascades for $\epsilon_{\mu\tau}$ and $\epsilon_{\tau\tau}$ | ✓ Tracks and cascades for all flavors   |
| × DC Monte Carlo from an older dataset                             | ✓ Data and Monte Carlo from DC 2018   | ✓ Reco $\rightarrow$ true mapping from Monte Carlo migration matrix                             |
| × 8 E bins from 6.3 eV <sup>2</sup> to 56 eV <sup>2</sup>          | ✓ 8 E bins from 5.6 eV <sup>2</sup> to 56 eV <sup>2</sup>                       | ✓ 8 E bins from 5.6 eV <sup>2</sup> to 56 eV <sup>2</sup>                                       |
| × 8 z bins from -1 to 0  | ✓ 8 z bins from -1 to 1   | ✓ 8 zenith angle bins from -1 to 1  |
| × Use "Overall" and "relative $\nu_e$ to $\nu_\mu$ " normalization | × Use "Overall" and "relative $\nu_e$ to $\nu_\mu$ " normalization              | ✓ Flux normalization uncertainty of 25%   |
| × Prior on spectral index  | × Prior on spectral index   | ✓ Zenith angle uncertainty of 4%  |
| × No zenith angle normalization                                    | × No zenith angle normalization   | ✓ No priors on oscillation parameters   |
| ✓ No priors on $\Delta m_{31}^2, \theta_{23}, \theta_{13}$         | ✓ No priors on $\Delta m_{31}^2, \theta_{23}$                                   | ✓ Marginalize $\Delta m_{31}^2$ and $\theta_{23}$ . All other oscillation parameters are fixed. |
|  | ✓ Fixes $\Delta m_{21}^2, \theta_{12}, \theta_{13}$                             |   |
|  | × Uncertainty on hadron production in atmosphere                                |   |
|  | × Uncertainty on neutrino nucleon cross section                                 |   |

- 
- [1] M. Honda et al., Calculation of atmospheric neutrino flux using the interaction model calibrated with atmospheric muon data. doi:10.1103/PhysRevD.75.043006.
- [2] A. M. Dziewonski and D. L. Anderson, Preliminary reference Earth model 25 (4) 297–356. doi:10.1016/0031-9201(81)90046-7.
- [3] IceCube Collaboration, All-sky point-source IceCube data: Years 2010-2012. doi:10.21234/B4F04V.
- [4] IceCube Collaboration, Search for sterile neutrinos with one year of IceCube data. URL <https://icecube.wisc.edu/data-releases/2016/06/search-for-sterile-neutrinos-with-one-year-of-icecube-data/>
- [5] M. G. Aartsen et al., Searching for eV-scale sterile neutrinos with eight years of atmospheric neutrinos at the IceCube Neutrino Telescope 102 (5) 052009. doi:10.1103/PhysRevD.102.052009.
- [6] IceCube Collaboration, Three-year high-statistics neutrino oscillation samples. doi:10.21234/ac23-ra43.
- [7] IceCube Collaboration et al., Measurement of Atmospheric Neutrino Oscillations at 6–56 GeV with IceCube DeepCore 120 (7) 071801. doi:10.1103/PhysRevLett.120.071801.
- [8] IceCube Collaboration 1 et al., Measurement of atmospheric tau neutrino appearance with IceCube DeepCore 99 (3) 032007. doi:10.1103/PhysRevD.99.032007.
- [9] I. Esteban et al., The fate of hints: Updated global analysis of three-flavor neutrino oscillations 2020 (9) 178. doi:10.1007/JHEP09(2020)178.
- [10] IceCube Collaboration, IceCube Upgrade Neutrino Monte Carlo Simulation. doi:10.21234/qfz1-yh02.
- [11] Bounds on non-standard interactions of neutrinos from IceCube DeepCore data - INSPIRE. URL <https://inspirehep.net/literature/1769239>
- [12] M. Maltoni and T. Schwetz, Testing the statistical compatibility of independent data sets 68 (3) 033020. arXiv:hep-ph/0304176, doi:10.1103/PhysRevD.68.033020.